

PAPER

View Article Online
View Journal | View Issue




Cite this: *Environ. Sci.: Adv.*, 2022, 1, 208

Received 20th March 2022
Accepted 8th April 2022

DOI: 10.1039/d2va00049k

rsc.li/esadvances

Carbon nanomaterial-based aerogels for improved removal of copper(II), zinc(II), and lead(II) ions from water

Darren M. Smith, Badri Hamwi and Reginald E. Rogers, Jr. *

Access to clean water continues to be an issue throughout the world. Carbon nanomaterials that were integrated into 2-D hybrid papers have previously shown the ability to adsorb metal ions, such as copper(II), and polyaromatics. The use of single-wall carbon nanotube–graphene nanoplatelet (SWCNT–GnP) aerogels with a 3-D architecture has led to increased adsorption of polyaromatic compounds. Herein we demonstrate their increased ability to adsorb copper(II), lead(II), and zinc(II) ions. Compared to SWCNT–GnP hybrid papers and activated carbon (AC), carbon nanomaterial (CNM)-based aerogels have an adsorption capacity, q , that is up to 5-fold, 7-fold, and 48-fold larger for copper, lead, and zinc, respectively.

Environmental significance

Supplies of freshwater have been decreasing due to population growth, natural disasters, and pollution. Advanced carbon-based technologies have allowed for opportunities with the advancement of efficient and cost-effective materials to quickly and easily remove contaminants from high demand drinking water areas. This work highlights the advantages of using carbon-based aerogels for removing metal ions, specifically copper, lead, and zinc, from water supplies.

1. Introduction

The continued exposure to transition and heavy metals, especially in developing countries, has the likelihood of becoming a critical problem due to the potential of these metals to be stored in the body and later distributed to vital organs.^{1,2} Metals can contaminate water streams through multiple sources such as storm-water run-off, industrial, agricultural, and mining activities, and natural sources.^{3–7} The development of public purified water systems has led to the need for regulation, given the impending impact on public health. In 1974, the United States Congress passed the Safe Drinking Water Act (SDWA), which allowed the Environmental Protection Agency (EPA) to set national health-based standards. In 1991, the Lead and Copper Rule (LCR) was created to reduce copper levels to <1.3 ppm; however, these regulations failed to prevent high levels of copper and lead contamination, such as in Detroit, MI public school drinking water in 2018.⁸

The need for purified drinking water has led to the development of techniques such as membrane filtration, reverse osmosis, and electrochemical methods;^{9–12} however, the speed and cost of large scale purification is still an issue.¹³ Adsorption-based technologies are considered to be low-cost and highly efficient pathways that are both promising and robust for the

purification of aqueous solutions.¹⁴ Adsorption techniques are sought after because of the ease of implementation and the capacity to remove contaminants, even at extraordinarily low concentrations.¹⁵ Adsorption can be a versatile method to remove a broad variety of organic and inorganic compounds, thus generating a point-of-use water purification with highly pure effluents. The mechanism of adsorption is a transient process where the undesired compounds move from a fluid phase to the surface of the adsorbent. The limiting factor in physisorption purification processes is the capacity of the adsorbent. In this process, the adsorbate will attach to the adsorbent through noncovalent interactions, such as van der Waals forces or π – π interaction.¹⁶ A stronger binding affinity between the adsorbate and the adsorbent allows for more layers of adsorbate to bind to the adsorbent. In order to increase the adsorption capabilities of adsorbents, the adsorbent must be able to be regenerated or have increased uptake.¹⁷

The unique properties of carbon nanomaterials (CNMs), such as nanotubes (CNTs) or graphene, have been studied as adsorbent additives for wastewater treatment.^{18–23} Activated carbon (AC) is the most widespread adsorbent; however, possessing open pore structures, high surface area, delocalized π electrons, and a hydrophobic surface allows CNTs to exhibit comparable or better adsorption capabilities.^{24–27} The preparation of nanohybrid materials, materials containing both graphene and CNTs, provides an efficient pathway toward superior adsorption nanostructures.²⁸ Recently, 2-dimensional

Department of Biomedical, Biological, and Chemical Engineering, University of Missouri, Columbia, MO, USA. E-mail: rrogers@missouri.edu



freestanding papers produced from CNTs and graphene nanoplatelets (GnPs) have shown higher adsorption uptake of Cu(II) than granular AC.²⁴ The combination of CNT–GnP hybrid papers has also shown enhanced adsorption of polyaromatics^{29,30} and pesticides¹⁷ with up to 39-fold increase compared to each component, or AC, alone. CNTs and CNT–GO hybrid materials have also demonstrated the ability to remove metal ions, such as Cu(II), from aqueous solutions.^{31–33} Recently, CNM-based aerogels have shown high binding affinity, almost double that of AC, for polyaromatics (2,4-dichlorophenoxyacetic acid and 1-pyrenebutyric acid).²⁹ The 3-D architecture of the aerogel has shown increased adsorption capacity, q , for polyaromatic compounds when compared to its 2-D counterpart.^{29,30} Utilizing a 3-dimensional construct, these aerogels function in a similar manner to a sponge resulting in rapid uptake of these organic contaminants from solution. The utility of these CNM-based aerogels towards the removal of heavy metal ions from aqueous systems has not been demonstrated up to this point. Showing a high binding affinity for metal ions would show the robustness of these types of aerogels for water purification.

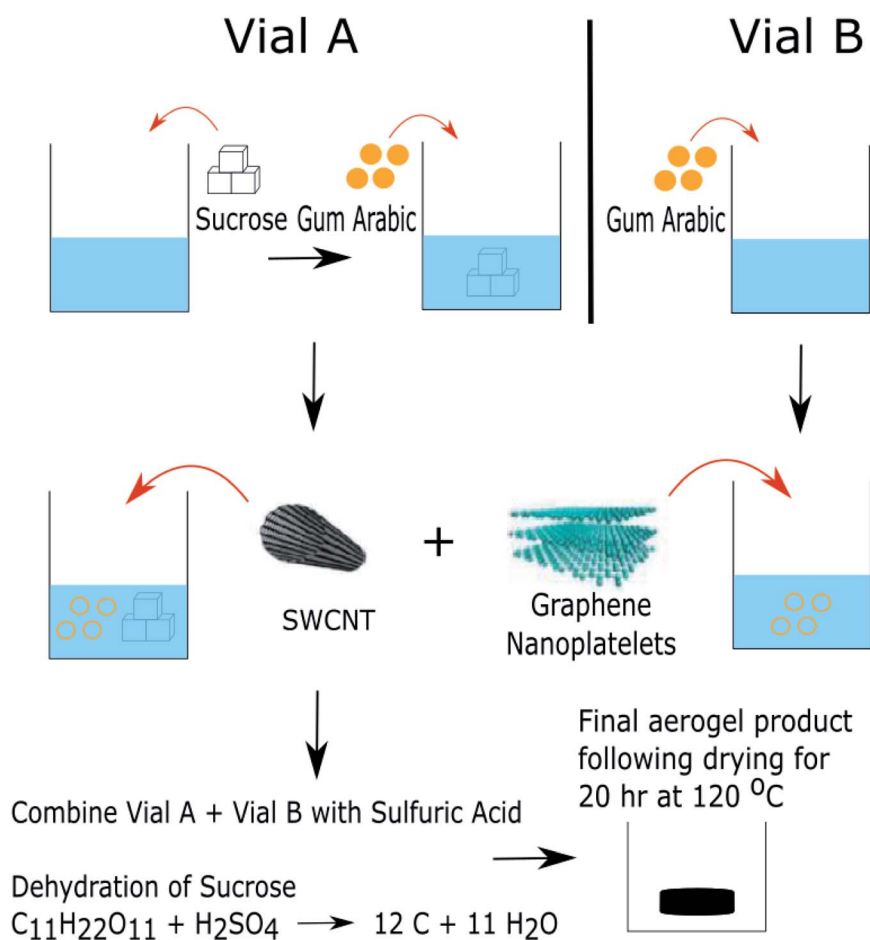
Here, the use of CNM-based aerogels for the removal of Cu(II), Pb(II), and Zn(II), using 3-D architecture structured aerogels integrated with GnPs and single-wall CNTs (SWCNTs), and how they functionally compare to SWCNT–GnP hybrid papers along

with AC, is demonstrated. The amorphous carbon aerogels contained CNM loadings of 0.2 and 2.0 wt%. The kinetic and equilibrium behavior of the aerogels towards the removal of metal ions was determined by batch adsorption experiments using UV-visible spectroscopy. CNM aerogels are shown to have a larger affinity towards the removal of metal ions from aqueous solutions than SWCNT–GnP hybrid papers and activated carbon.

2. Materials and methods

2.1 Preparation of carbon nanomaterial (CNM)-based aerogels

The preparation of carbon nanomaterial (CNM)-based aerogels was completed analogous to previous work.²⁹ Scheme 1 shows the CNM aerogel preparation, in which approximately 2.5 grams of sucrose (certified A.C.S., Fisher Chemical) was dissolved in 5 mL of deionized (DI) water (1.5 μ S) in a 20 mL scintillation vial labeled “A”. The solution was ultrasonicated at room temperature for 60 minutes to aid in dissolution. After initial sonication, gum arabic (Pure Supplements Co., USA) was then added to vial “A” and a different 20 mL scintillation vial, labeled “B”, based on Table 1. Gum arabic has been shown to aid in non-aggregation of the carbon materials in aqueous solutions.³⁴ The scintillation vials were then sonicated for 30 min at room temperature to



Scheme 1 Preparation process for carbon nanomaterial-based aerogels.



Table 1 Mass contents of gum arabic (mg) and carbon nanomaterials (mg) used for aerogel preparation

Weight% loading	Scintillation vial A		Scintillation vial B	
	Gum arabic	Carbon nanomaterial	Gum arabic	Carbon nanomaterial
0	17	0	33	0
0.2	17	1.7	33	3.4
2	34	17	66	34

unwind the gum arabic chains. Carbon nanomaterials were added to both of the scintillation vials based on the desired carbon nanomaterial loading listed in Table 1. Single-wall carbon nanotubes (SWCNTs, 90%, Carbon Solutions, Inc., length: 0.5–3 μm and diameter: 0.8–1.6 μm) and graphene nanoplatelets (GnPs, 96%, Global Graphene Group, length: 7 μm and thickness: 30–50 nm) had previously been soaked in concentrated hydrochloric acid (HCl, 37.5% Sigma-Aldrich) for 17 hours, to remove metal particles, then vacuum filtered through a 47 mm, 0.22 μm filter and thoroughly washed with DI water. The GnPs and SWCNTs were dried in a vacuum oven for 20 h at 120 $^{\circ}\text{C}$, at ambient pressure, prior to use in aerogel preparation. Aerogels were prepared with varying mass contents of carbon nanomaterial (SWCNTs and GnPs), 0.2 wt% and 2.0 wt%, with a previously utilized mass ratio of 1 : 1 (SWCNTs : GnPs). This mass ratio of SWCNTs to GnPs showed the most optimal removal of contaminants compared to other weight ratios.²⁹ The resulting solution was dispersed by sonication at room temperature for 60 minutes. Following the final sonication, vial “A” was poured into a 150 mL beaker. Vial “B” and 10 mL of sulfuric acid (93% by weight, Fisher Chemical) were simultaneously poured into the beaker holding the contents from vial “A”. An exothermic reaction was immediately observed, resulting in the formation of the aerogel in the beaker. The beaker was allowed to cool for 5 minutes to allow for safe handling prior to removing excess liquid by transfer pipet. The resulting aerogel was transferred to a new beaker and soaked in approximately 200 mL of deionized water for 12 hours. The water was then decanted from the beaker and the aerogel was dried in a vacuum oven at 120 $^{\circ}\text{C}$, under ambient pressure, for 20 hours.

2.2 Batch adsorption sample preparation process

The cylindrical shaped CNM aerogels were removed and placed on a platform similarly to their orientation in the beaker. The aerogel was then cut into three even sections: left, middle, and right as shown in Fig. 1. The sulfuric acid catalyzed dehydration of sucrose allowed for the random dispersion of the CNM throughout the aerogel material. Batch adsorption studies were performed on three samples from each section to determine the uniformity of adsorption throughout the entire aerogel. Average aerogel sample masses used for the solutions were 21.3 ± 0.9 , 20.8 ± 0.5 , and 20.5 ± 0.7 mg for Cu(II), Zn(II), and Pb(II) nitrate solutions, respectively.

2.3 Adsorbate solution preparation

Adsorbate solutions were prepared at concentrations of 0.5 mg mL^{-1} and 0.1 mg mL^{-1} by adding the appropriate amount of cupric nitrate hemi(pentahydrate) (98.9%, Fisher Chemical), zinc(II) nitrate hexahydrate (98.0%, Acros Organics), and lead(II) nitrate (>99%, Sigma Aldrich) to a volumetric flask and dissolving in deionized water.

2.4 Adsorption measurements

Batch adsorption studies were performed by using three samples from each of the three layers of every aerogel (left, middle, and right) and placing them in 20 mL scintillation vials with 10 mL of the adsorbate solution. These studies were completed on aerogels containing differing amounts of carbon nanomaterials: 0.2 wt% and 2.0 wt%. Short-term adsorption studies and measurements of equilibrium concentrations of the batch systems were

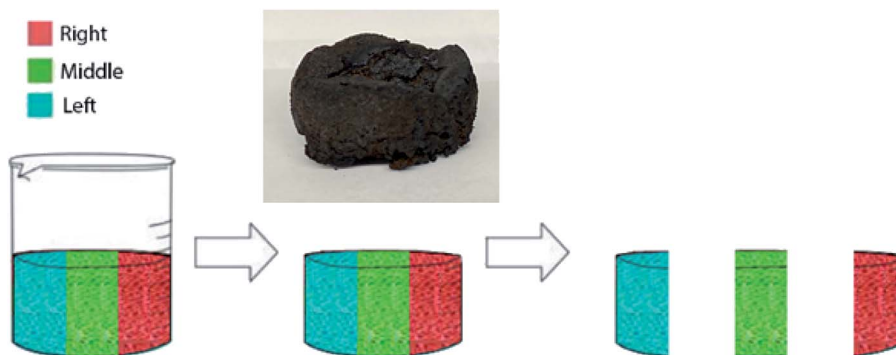


Fig. 1 Illustration demonstrating how the CNM aerogel is removed from the beaker and sectioned for study. The inset is an image of a fully prepared and dried CNM aerogel.



performed in 15 min intervals. Absorbance measurements were taken on a PerkinElmer Lambda 950 UV/Vis/NIR spectrometer by placing approximately 3 mL of each solution in a quartz cuvette (Cu(II) $\lambda = 635$ nm, Zn(II) $\lambda = 218$ nm, Pb(II) $\lambda = 215$ nm).³⁵ The scintillation vials containing the adsorbate solutions and the aerogel samples were placed on an orbital shaker (Vevor, B07B3LLJT7) and continuously agitated for 15 min at 120 rpm. The uptake of the agitated solutions was calculated in 15 min intervals, for a total of eight intervals (120 min), by measuring the change in absorption over time. A mass balance on the bulk solution was used to calculate all adsorption capacities, q (see Section 3.2 for further explanation on q).

3. Results and discussion

3.1 CNM aerogel characterization

The inset in Fig. 1 shows an example of a completely prepared CNM aerogel prior to use. The density of 0.2 wt% and 2.0 wt% aerogels was estimated to be 0.626 to 0.952 g mL⁻¹, respectively. We have previously reported a density of 0.414 g mL⁻¹ for 0.0 wt% aerogel.²⁹ This shows that as the wt% of CNM in the aerogel increases, the density also increases, but at a decreasing rate. Compared to other aerogel materials, these CNM aerogels have a much higher density.^{36,37} The overall structural integrity of the aerogels does not change significantly over different periods of time. In terms of mechanical stability, the variation in the density of the aerogel due to different weight loadings of CNMs does not cause the aerogel to collapse. Instead, it is observed that the aerogel holds its structure even after application of small pressures (*i.e.* holding the aerogel with tweezers or hands). Such stability is critical for further advancing the use of these aerogels in applications involving continuous flow systems where pressure forces will need to be taken into account.

3.2 pH measurements of copper(II), zinc(II), and lead(II) nitrate solutions

In order to compare the performance of the 3-D architecture to other adsorption media, 0.5 mg mL⁻¹ and 0.1 mg mL⁻¹

Table 3 List of copper(II) solutions for pH study with amounts of 0.1 M NaOH (μL) added to each solution to obtain the given pH

Sample	0.1 M NaOH	pH
1	10	5.41
2	20	5.61
3	30	5.82
4	40	5.98
5	50	6.12
6	60	6.19
7	100	6.26
8	500	6.66
9	550	7.12
10	600	9.12

solutions of metal(II) nitrate were prepared. Since precipitation of metal salts would lead to erroneous conclusions resulting from higher than actual adsorption calculations, the pH of the solutions was tested throughout the batch adsorption study with pH values being as low as 2.18 and 2.28 for the 0.5 mg mL⁻¹ and 0.1 mg mL⁻¹ copper solutions, respectively.

The starting DI water had a pH of 5.7. Table 2 shows the decrease in pH of the solution with increasing copper(II) nitrate concentration from 4.84 (0.1 mg mL⁻¹) to 4.05 (20 mg mL⁻¹). The starting pH of 0.5 mg mL⁻¹ and 0.1 mg mL⁻¹ copper(II) nitrate solutions were 4.71 and 4.84, respectively.

Once the aerogel was added to the pH 5.7 DI water, the pH dropped to 1.99. This is due to residual acid in the aerogel from preparation. In order to determine the pH at which Cu(II) salts precipitate, 10 mL of 0.5 mg mL⁻¹ Cu(II) solution was put into scintillation vials and required amounts of 0.1 M NaOH were added to achieve the desired pH. Fig. 2 shows an array of copper(II) nitrate solutions with pH given in Table 3, along with the amounts of 0.1 M NaOH required. While aggregated precipitation was not seen until a pH of 9.12, the solution began turning blue in color at a pH of 6.19, showing non-aggregated precipitation from solution. Table 4 shows that the pHs of the batch study remained below a pH of 2.3, which demonstrates that all the removal of Cu(II) from solution is from uptake into the adsorbent.

The pH of zinc and lead nitrate solutions was tested at equivalent concentrations. The starting pH of 0.5 mg mL⁻¹ and 0.1 mg mL⁻¹ zinc(II) nitrate solutions were 4.3 and 5.1, respectively, while the starting pH of 0.5 mg mL⁻¹ and 0.1 mg mL⁻¹ lead(II) nitrate solutions were 4.3 and 4.7, respectively. Table 5 gives a summary of the pHs of all metal ion solutions. Since the starting pH for zinc(II) nitrate and lead(II) nitrate solutions are similar to the pH of the copper(II) nitrate solutions, it is

Table 2 pH of copper(II) nitrate solutions at given concentrations

Concentration (mg mL ⁻¹)	pH
0.1	4.84
0.5	4.71
5.0	4.46
10	4.28
20	4.05

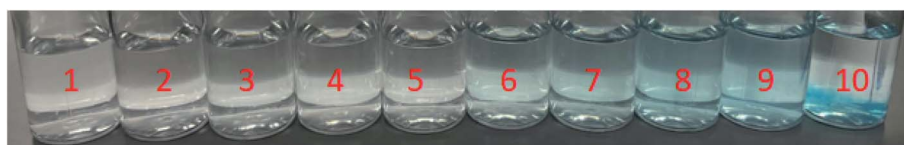


Fig. 2 pH study of 0.5 mg mL⁻¹ copper(II) nitrate. The pH of the solutions ranged from 5.41 to 9.12 (left to right).



Table 4 pH results from the kinetic test with adsorbent 0.2 wt% and 2.0 wt% aerogels and adsorbate 0.5 mg mL⁻¹ and 0.1 mg mL⁻¹ copper(II) nitrate solutions

Time (min)	pH of 0.5 mg mL ⁻¹		pH of 0.1 mg mL ⁻¹	
	0.20 wt%	2.00 wt%	0.20 wt%	2.00 wt%
15	2.18	2.02	2.28	2.06
30	2.18	2.02	2.28	2.06
45	2.18	2.01	2.27	2.06
60	2.17	2.00	2.27	2.04
75	2.16	1.99	2.27	2.04
90	2.17	1.99	2.26	2.04
105	2.17	1.99	2.26	2.04
120	2.16	1.99	2.26	2.04

Table 5 pH data for starting metal ion solutions at list concentration

	Cu(II)	Zn(II)	Pb(II)
0.5 mg mL ⁻¹	4.71	4.30	4.30
0.1 mg mL ⁻¹	4.84	5.10	4.70

presumed that the metal ions will precipitate at a similar pH to that of copper(II) nitrate.

3.3 Batch adsorption studies

The time dependent adsorption of 0.5 mg mL⁻¹ and 0.1 mg mL⁻¹ copper(II), zinc(II), and lead(II) nitrate solutions can be observed in Fig. 3–5, respectively. A mass balance on the bulk solutions was used to calculate all adsorption capacities, q .

$$q = V(C_o - C_t)/M_{\text{adsorbent}} \quad (1)$$

The adsorption capacity is described in eqn (1) where the concentration (mg mL⁻¹) of the metal ion in solution at a given time t is C_t (C_o , initial concentration). The volume, V , of the

solution is held constant at 10 mL, and the mass of the adsorbent, $M_{\text{adsorbent}}$, is in grams.

As observed in Fig. 3a, the difference in uptake between the different systems is clearly visible as the aerogel's sponge-like structure yields a much more rapid adsorption of the adsorbate than the 2-D hybrid paper or AC. The adsorption of Cu(II) onto the aerogel follows a pseudo-second order kinetic model,^{17,38} increasing at a constant rate until approximately 75 minutes, where the adsorption capacity slows and finally reaches equilibrium at around 105 minutes for the 2.0 wt% and 90 minutes for the 0.2 wt% aerogel, while the hybrid paper has a low linear adsorption and does not reach a maximum during the 120 min time interval of the experiment and AC had negligible uptake of the Cu(II) ions. The initial increase is due to the interaction of the open valence of the Cu(II) ions and the π network of the CNM. The latter stages of the experiment are where the π network is fully coordinated with Cu(II), saturating the CNM aerogel, and thus equilibrium is reached. The adsorption of Cu(II) onto the 3-D structure of the aerogel showed a much larger adsorption capacity, q , than the 2-D hybrid papers and AC. The increased amounts of CNM aerogel allowed for increased uptake of the Cu(II) ions, shown by the 2.0 wt% aerogel having a q that is ~ 30 mg adsorbate per gram of adsorbent higher than the 0.2 wt% aerogel. The result of the larger adsorption capacity of the aerogel, compared to the hybrid papers, is due to the larger surface area to volume ratio of the material.²⁹ The sponge-like structure, allowing for a larger surface area, of the aerogel allows for more adsorption sites for the copper ions to bind to the CNM. This also allows for a better distribution of the CNM throughout the adsorbent material.

Fig. 3b shows a time dependent adsorption of the 0.1 mg mL⁻¹ copper(II) nitrate solution onto 0.2 and 2.0 wt% CNM aerogels, 2-D hybrid paper, and AC. The adsorption capacity is linear for the aerogel until 75 minutes where the aerogel begins to increase. The hybrid papers follow a similar pathway to the aerogels but the increase from the baseline is delayed until approximately 105 minutes, compared to 75 minutes for the aerogels. The 0.2 wt% and 2.0 wt% CNM aerogel has

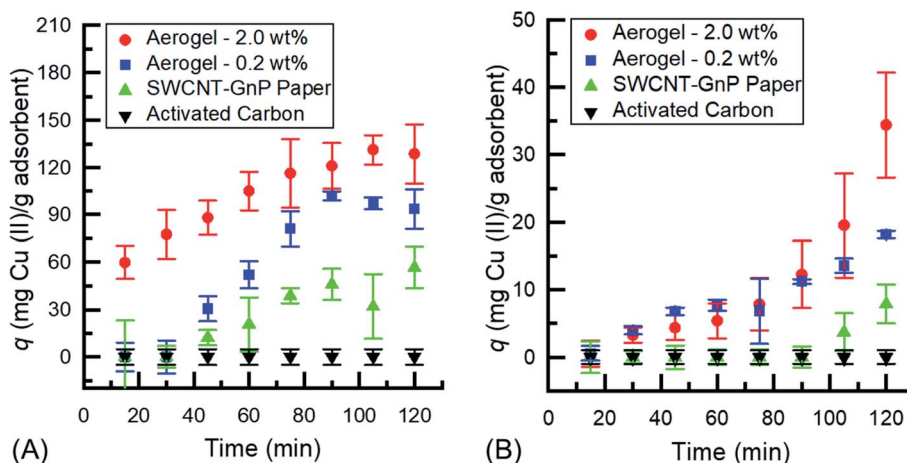


Fig. 3 Time dependent adsorption for removal of adsorbate (Cu(II)) with initial concentrations of (A) 0.5 mg mL⁻¹ and (B) 0.1 mg mL⁻¹ by carbon nanomaterial (CNM)-based aerogels of (●) 2.0 wt% and (■) 0.2 wt%, (▲) SWCNT-GnP hybrid paper, and (▼) activated carbon.



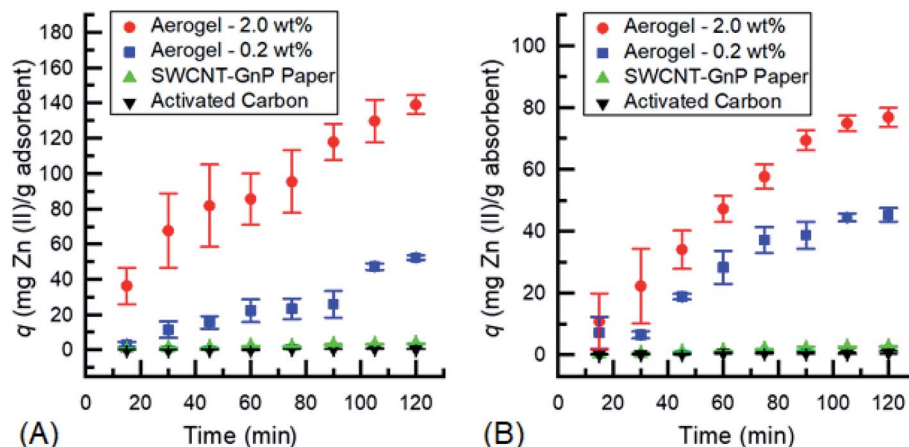


Fig. 4 Time dependent adsorption for removal of adsorbate (Zn(II)) with initial concentrations of (A) 0.5 mg mL^{-1} and (B) 0.1 mg mL^{-1} by carbon nanomaterial (CNM)-based aerogels of (●) 2.0 wt% and (■) 0.2 wt%, (▲) SWCNT-GnP paper, and (▼) activated carbon.

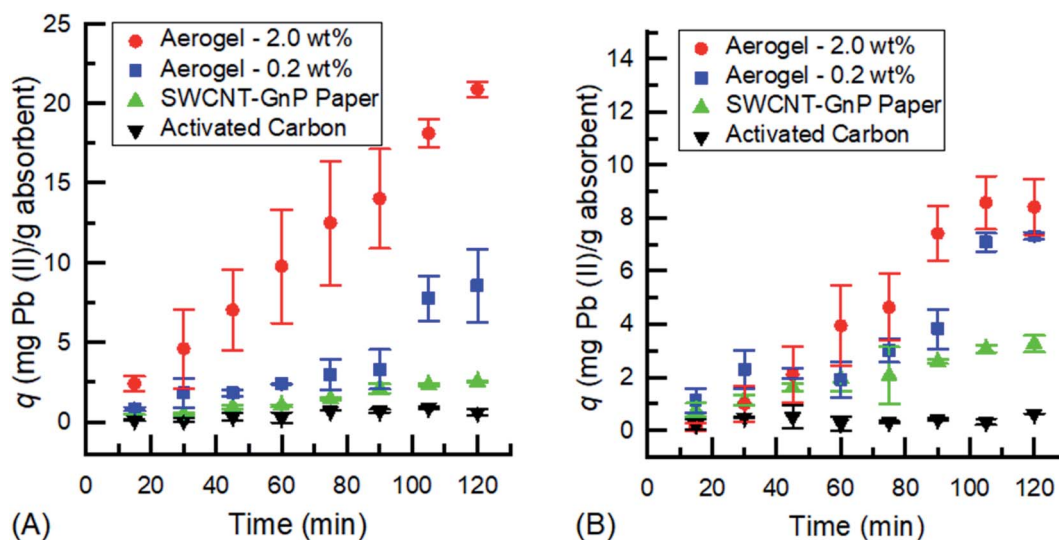


Fig. 5 Time dependent adsorption for removal of adsorbate (Pb(II)) with initial concentrations of (A) 0.5 mg mL^{-1} and (B) 0.1 mg mL^{-1} by carbon nanomaterial (CNM)-based aerogels of (●) 2.0 wt% and (■) 0.2 wt%, (▲) SWCNT-GnP hybrid paper, and (▼) activated carbon.

a maximum $q \approx 18$ and $35 \text{ mg adsorbate per gram adsorbent}$, respectively, while for the hybrid papers $q < 10 \text{ mg adsorbate per gram adsorbent}$ and AC q is negligible. This shows that the 3-D structure of the aerogels allows for a more rapid uptake of Cu(II) ions compared to the 2-D hybrid papers and AC. Unlike the 0.5 mg mL^{-1} solution, shown in Fig. 3a, none of the samples reached a plateau in adsorption uptake capacity for the 0.1 mg mL^{-1} solution during the 120 min time range. It is believed that the low concentration of copper ions at 0.1 mg mL^{-1} has a slower uptake by the aerogel based on the interaction between the copper and aerogel. Given the concentration is five times less than the initial concentration of 0.5 mg mL^{-1} , there is a slower ramp up time that can be attributed to the diluted state of the solution and the slower interaction time between the copper and the aerogel. To prove this hypothesis the experiments were run for 240 minutes. The 0.1 mg mL^{-1} Cu(II)

solution reached equilibrium at 120 minutes, 30 minutes after the 0.5 mg mL^{-1} Cu(II) solution reached equilibrium.

In Fig. 4a, Zn(II) is observed to follow a trend similar to the Cu(II) results. The uptake in both aerogels was significantly higher than that of the 2-D hybrid papers and AC. The 2.0 wt% aerogel had a seemingly larger uptake capacity than the 0.2 wt% aerogel with a maximum q that is $\sim 90 \text{ mg adsorbate per gram of adsorbent}$ higher. While neither aerogel seems to have reached an absolute maximum due to the absence of a clear plateau in the uptake capacity, the 2.0 wt% aerogel could be considered to have peaked with regard to the low standard deviation at 120 min as well as an insignificant difference in uptake from 105 min. Further experiments for 240 minutes showed that the 2.0 wt% CNM aerogel with 0.5 mg mL^{-1} Zn(II) solution did reach saturation at the 120 minute mark. On the other hand, due to the large difference in uptake of both aerogels compared to that of the 2-D hybrid paper and AC, the uptake capacity of the 2-D



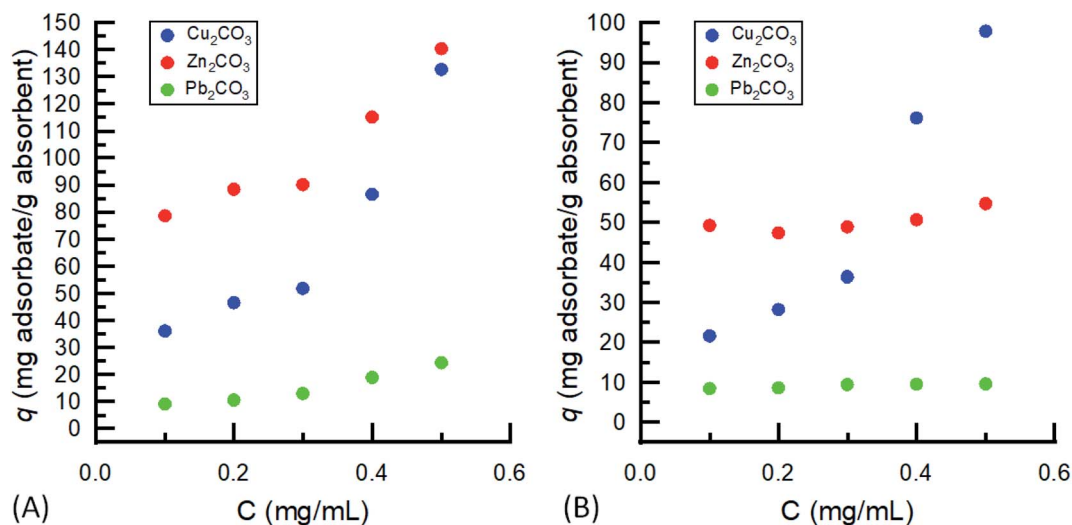


Fig. 6 Concentration dependent adsorption for removal of adsorbate ((●) Cu(II), (●) Zn(II), and (●) Pb(II)) at time 120 minutes by (A) 2.0 wt% and (B) 0.2 wt% carbon nanomaterial (CNM)-based aerogels.

hybrid papers and AC is negligible. Fig. 4b in contrast is more consistent with its trend to that of the Cu(II) results in Fig. 3a, specifically in terms of following a pseudo-second order kinetic model^{17,38} and also reaching certain maxima. The uptake of both types of aerogels, 2.0 wt% and 0.2 wt%, clearly reaches an equilibrium after a maximum q of 70 mg adsorbate per gram of adsorbent for the 2.0 wt% aerogel at the 90 minute mark and a q of 40 mg adsorbate per gram of adsorbent for the 0.2 wt% aerogel at the 75 minute mark. An important point to note is that the difference between the maximum uptake capacities of the two aerogels is about 30 mg adsorbate per gram of adsorbent, with the 2.0 wt% aerogel having the highest uptake of the four types of adsorbents used in this study. Moreover, the uptake capacities of the 2-D hybrid papers and AC in the 0.1 mg mL⁻¹ Zn(II) solution are below 5 mg adsorbate per gram of adsorbent which makes them relatively insignificant.

Fig. 5 demonstrates the uptake capacities of the four adsorbents for Pb(II) ions. With a generally similar trend to the previous adsorption results of the Cu(II) and Zn(II) metal ions, it is noticeably lower in average uptake capacity within the 120 minute study window. This is due to Pb(II)'s significantly larger molecular weight (MW) and ionic radius (IR) (MW/IR = 207.2/119 pm) compared to those of Cu(II) and Zn(II) (63.6/73 pm and 65.4/74 pm, respectively). These factors significantly affect the adsorption kinetics due to the direct correlation of uptake capacity and binding sites, making it harder to adsorb as many Pb(II) ions as Cu(II) and Zn(II). Fig. 5a shows that the 2.0 wt% aerogel does not reach a maximum uptake capacity compared to the 0.2 wt% aerogel and 2-D hybrid paper, which reach their maxima at the 105 minute mark. However, it is important to note that the equilibrium uptake capacity for the 2.0 wt% aerogel, which comes at the 120 minute mark, seen in the 240 minute experiment, is about 3 times larger than that of the 0.2 wt% aerogel and almost 10 times larger than that of the 2-D hybrid paper. Fig. 5b exhibits similar behavior to Fig. 5a with the exception of the 2.0 wt% aerogel as it reaches a maximum at

the 90 minute mark with a plateau in adsorption capacity. It is also closer in its maximum uptake to the 0.2 wt% aerogel, both being within a ~2 mg adsorbate per gram of adsorbent range. While the 2-D hybrid papers display a slightly higher maximum uptake, approximately ~3 mg adsorbate per gram of adsorbent, than the previous 2-D hybrid paper results in Fig. 5, activated carbon remains within the negligible uptake capacity region. Overall, the 0.1 mg mL⁻¹ Pb(II) solution results in Fig. 5b reveal lower average uptake capacities due to the lower concentration of the solution.

Equilibrium isotherms, Fig. 6, were created using the data at 120 minutes for each concentration at 0.1 mg mL⁻¹ intervals from 0.5 mg mL⁻¹ to 0.1 mg mL⁻¹. As seen in the previous sections, Pb(II) was observed to have the smallest uptake due to the much larger atomic radius, although the increased amount of CNM (2.0 wt%) within the aerogels showed an exponential increase in uptake capacity over the 0.2 wt% aerogel, which was rather linear. The adsorption of Zn(II) onto the CNM aerogel possessed a similar pattern to Pb(II), although Zn(II) was over three times more active at being adsorbed. The CNM aerogels showed the greatest ability to adsorb Cu(II) with both the 2.0 and 0.2 wt% aerogels adsorbing Cu(II) in an exponential manner as the concentration of the metal ion increased. For all three metals studies, the equilibrium isotherms showed a primarily linear behavior as opposed to behavior most common of Langmuir or Freundlich-type models.³⁹

4. Conclusion

In summary, we have presented the preparation and use of CNM aerogels for Cu(II), Zn(II), and Pb(II) ion removal from aqueous solutions. We demonstrated that utilizing a 3-D CNM aerogel increased the adsorption capacity for these metal ions compared to 2-D hybrid paper and AC by as much as 48-fold, even though equilibrium was not observed by all of the CNM aerogels in the 120 min timeframe. The q values of the 2.0 wt%



aerogel were greater than, or equal to, twice that of the 0.2 wt% aerogel in both the 0.5 mg mL⁻¹ and 0.1 mg mL⁻¹ solutions. The only exception to this result was the 0.1 mg mL⁻¹ Pb(II) solution, where 2.0 wt% and 0.2 wt% aerogels had approximately similar *q* values. The pH of the metal(II) ion solutions were also tested to demonstrate that the removal of metal ions was solely from adsorbent uptake and not precipitation from solution, which did not happen until solution pH > 6.19. The 3-D architecture has previously shown a greater ability to take up polyaromatics from aqueous solutions than AC.²⁹ Here we have shown the ability of the aerogels to also remove metal ions from aqueous solutions. This indicates the future potential of CNM aerogels to be adsorbents for complete water purification.

Conflicts of interest

The authors declare no conflicting interest.

Acknowledgements

The authors would like to thank the College of Engineering and Paul F. Roth Fund for Faculty Excellence for financial support during the course of this project. The financial support agencies had no involvement in the study design; in the collection, analysis and interpretation of data; in the writing of this report; and in the decision to submit the article for publication. The authors would also like to thank Andrew Maggard and Luke Biehn for use of their 2-D hybrid papers.

References

- 1 H. H. An, M. Luchak and R. Copes, *Clin. Toxicol.*, 2015, **53**, 757.
- 2 V. Hrdlička, M. Choiniska, B. R. Redondo, J. Barek and T. Navrátil, *Electrochim. Acta*, 2020, **354**, 136623.
- 3 K. R. Reddy, T. Xie and S. Dastgheibi, *J. Environ. Chem. Eng.*, 2014, **2**, 282.
- 4 M. D. Kaminski and S. Landsberger, *J. Air Waste Manage. Assoc.*, 2000, **50**, 1667.
- 5 V. Masindi and K. L. Muedi, in *Heavy Metals*, IntechOpen, Aglan, France, 2018, p. 115.
- 6 J. Gunawardena, P. Egodawatta, G. A. Ayoko and A. Goonetilleke, *Atmos. Environ.*, 2013, **68**, 235.
- 7 S. Iram, I. Ahmad and D. Stuben, *Pak. J. Bot.*, 2009, **41**(2), 885.
- 8 F. Karimi and J. DiGiacomo, CNN: Health, September 20, 2018, <https://www.cnn.com/2018/09/20/health/detroit-schools-water-lead-copper/index.html>, accessed on February 19, 2021.
- 9 M. A. Shannon, P. W. Bohn, M. Elimelech, J. G. Georgiadis, B. J. Mariñas and A. M. Mayes, *Nature*, 2008, **452**, 301.
- 10 R. I. L. Eggen, J. Hollender, A. Joss, M. Scharer and C. Stamm, *Environ. Sci. Technol.*, 2014, **48**, 7683.
- 11 M. G. Buonomenna, *RSC Adv.*, 2013, **3**, 5694.
- 12 M. M. Pendergast and E. M. V. A. Hoek, *Energy Environ. Sci.*, 2011, **4**, 1946.
- 13 A. B. Dichiaro, S. J. Weinstein and R. E. Rogers Jr, *Ind. Eng. Chem. Res.*, 2015, **54**, 8579.
- 14 I. Ali and V. K. Gupta, *Nat. Protoc.*, 2007, **1**, 2661.
- 15 E. L. Cussler, *Diffusion: Mass Transfer in Fluid System*, Cambridge University Press, Cambridge, U. K., 2009, p. 436.
- 16 D. Borodin, I. Rahinov, P. R. Shirhatti, M. Huang, A. Kandratsenka, D. J. Auerbach, T. Zhong, H. Guo, D. Schwarzer, T. N. Kitsopoulos and A. M. Wodke, *Science*, 2020, **369**(6510), 1461.
- 17 A. B. Dichiaro, J. Benton-Smith and R. E. Rogers Jr, *Environ. Sci.: Nano*, 2014, **1**, 113.
- 18 X. Qu, P. J. J. Alvarez and Q. Li, *Water Res.*, 2013, **47**, 3931.
- 19 M. Khaljeh, S. Laurent and K. Dastafkan, *Chem. Rev.*, 2013, **113**, 7728.
- 20 D. V. Kazachkin, Y. Nishimura, S. Irle, X. Feng, R. Vidic and E. Borguet, *Carbon*, 2010, **48**, 1867.
- 21 R. E. Rogers Jr, T. I. Bardsley, S. J. Weinstein and B. J. Landi, *Chem. Eng. J.*, 2011, **173**, 486.
- 22 J. Jin, R. Li, H. Wang, H. Chen, K. Liang and J. Ma, *Chem. Commun.*, 2007, **4**, 386.
- 23 K. C. Kemp, H. Seema, M. Saleh, N. H. Le, K. Mahesh, V. Chandra and K. S. Kim, *Nanoscale*, 2013, **5**, 3149.
- 24 A. B. Dichiaro, M. R. Webber, W. R. Gorman and R. E. Rogers Jr, *ACS Appl. Mater. Interfaces*, 2015, **7**, 15674.
- 25 C. H. Wu, *J. Colloid Interface Sci.*, 2007, **311**, 338.
- 26 J. Wang, Z. Li, S. Li, W. Qi, P. Liu, F. Liu, Y. Ye, L. Wu, L. Wang and W. Wu, *PLoS One*, 2013, **8**, e72475.
- 27 Ş. S. Bayazit and İ. İnci, *J. Mol. Liq.*, 2014, **199**, 559.
- 28 H. Wang, H. Ma, W. Zheng, D. An and C. Na, *ACS Appl. Mater. Interfaces*, 2014, **6**, 9426.
- 29 B. S. Litts, M. K. Eddy, P. M. Zaretsky, N. N. Ferguson, A. B. Dichiaro and R. E. Rogers Jr, *ACS Appl. Nano Mater.*, 2018, **1**(8), 4127.
- 30 A. B. Dichiaro, T. J. Sherwood and R. E. Rogers Jr, *J. Mater. Chem. A*, 2013, **1**, 14480.
- 31 A. Stafiej and K. Pyrzyńska, *Sep. Purif. Technol.*, 2007, **58**, 49.
- 32 M. Musielak, A. Gagor, B. Zawisza, E. Talik and R. Sitko, *ACS Appl. Mater. Interfaces*, 2019, **11**, 28582.
- 33 L. Chaabane, E. Beyou, A. E. Ghali and M. H. V. Baouab, *J. Hazard. Mater.*, 2020, **389**, 121839.
- 34 M. T. Kim, H. S. Park, D. Hui and K. Y. Rhee, *J. Nanosci. Nanotechnol.*, 2011, **11**, 7369.
- 35 Illinois Central College: Chemistry 130 Lab: Beer's Law: Colorimetry of Copper(II) Solutions, <https://faculty.icc.edu/bcook/30XP11VB.pdf>, accessed December 2020.
- 36 M. Dilamian and B. Noroozi, *Carbohydr. Polym.*, 2021, **251**, 117016.
- 37 X. Zhang, Z. Chen, J. Zhang, X. Ye and S. Cui, *Chem. Phys. Lett.*, 2021, **762**, 138127.
- 38 Y. S. Ho and G. McKay, *Process Biochem.*, 1999, **34**, 451.
- 39 E. L. Cussler, *Adsorption: Isotherms, Diffusion: Mass Transfer in Fluid Systems*, Cambridge University Press, 3rd edn, 2017, pp. 428–430.

